Heliyon 5 (2019) e01698

Contents lists available at ScienceDirect

Heliyon

journal homepage: www.heliyon.com

Evaluation of mandibular calcification on 3D volume images

Barbara Schreiner-Tiefenbacher, Vivian Forster, Klaudio Pauli, Walter Sutter, Marius Meier, Henning Roland, Patrick Bandura, Dritan Turhani *

Centre for Oral and Maxillofacial Surgery, University of Dental Medicine and Oral Health, Danube Private University (DPU), Krems, Austria

ARTICLE INFO

Keywords:
Dentistry
Medical imaging

ABSTRACT

Objectives: Bone and soft-tissue calcifications are often coincidentally diagnosed on digital panoramic radiographs (DPRs). As the use of three-dimensional (3D) images has increased in the past decade for diagnostics in the mandibular region, we evaluated 3D volume images derived from 2D panoramic images to determine if this method is suitable for early detection of calcifications in this region.

Methods: In this study, three investigators retrospectively and independently evaluated 822 DPRs. If one or more calcifications were present, the 3D volume image from that patient was retrospectively evaluated to confirm the incidental findings. A radiographic system with a low-dose mode and a high-resolution 3D-image function was used. The investigators focussed on the most common calcifications, including tonsilloliths (TL), idiopathic osteosclerosis (IO) of the mandible, carotid artery calcifications (CAC), calcified submandibular lymph nodes (hereafter, CSL), and sialoliths of the submandibular salivary gland (SSG).

Results: One or more calcifications were identified in 415 (50.5%) DPRs. In total, 718 calcifications were detected, 30.2% of which were TL, 16.3% IO, 11.3% CAC, 8.8% CSL, and 1.7% SSG. Only 287 (39.97 %) of the calcifications were confirmed on 3D volume images; of these, 29.2% were TL, 58.5% IO, 0.2% CAC, and 1.4% SSG. No CSLs were detected.

Conclusions: Not all areas shown on the DPRs were visible in the retrospectively obtained 3D volume images. Whereas DPRs are used to diagnose calcifications such as IO, TL, SSG, CAC, and CSL, the 3D volume images were only useful for confirming the existence of IO, TL, and SSG calcifications.

1. Introduction

The most common calcifications in the mandibular region are tonsilloliths (TL), sialoliths of the submandibular salivary gland (SSG), carotid artery calcifications (CAC), calcified submandibular lymph nodes (hereafter referred to as CSL), and idiopathic osteosclerosis (IO) [1, 2, 3, 4]. As these calcifications are often detected on two-dimensional (2D) digital panoramic radiographs (DPRs), verification of their presence using 3D volume images may allow for an early diagnosis [5].

The DPR is the most important initial diagnostic tool in dentistry and is used primarily to determine a patient's overall dental health status [6]. The jaw, maxillary sinus, nasal cavity, teeth, roots of the teeth, spine (to some extent), and several types of soft-tissue calcification can be examined using a DPR [7, 8, 9]. In recent years, cone-beam computed tomography (CBCT) has increased a physician's ability to diagnose soft-tissue calcifications in the head and neck region [10]. CBCT 3D scans allow for a maximum field of view (FOV) with a low radiation dose, which was previously only possible with computed tomography (CT) or nuclear spin tomography [5, 11]. This provides new possibilities for diagnostics in the alveolar ridge and surrounding areas, as well as evaluation of specific structures, including certain types of calcification [3, 12, 13, 14]. The potential of 3D volume images has not yet been completely realized [15], and the limits of this imaging technique in the mandibular region have not been fully evaluated [16, 17, 18, 19, 20].

Data collected using the Orthophos SL 3D imaging unit (Dentsply Sirona, York, PA, USA) was used to obtain information from 2D and 3D volume panoramic views with a single dose of radiation. The features of this system include a direct conversion sensor, sharp-layer technology, and an adjustable FOV [15]. The time required to generate a 3D image of the jaw using the Orthophos SL 3D is equal to that required to prepare a 2D DPR. The Orthophos SL 3D has the advantage of lower radiation exposure, which makes it possible to diagnose structures that can be detected but not confirmed with DPRs [13]. The aim of this study was to determine whether the same areas on a DPR can be evaluated on 3D

* Corresponding author.
E-mail address: Dritan.Turhani@DP-Uni.ac.at (D. Turhani).

https://doi.org/10.1016/j.heliyon.2019.e01698
Received 15 November 2018; Received in revised form 22 March 2019; Accepted 7 May 2019

Table 1
Frequencies of calcifications.

Parameter		Male		Female		Total	
		DPR	3D	DPR	3D	DPR	3D
TL	Left	37	19	33	16	70	35
	Right	21	14	45	32	66	46
	Bilateral	46	14	67	26	113	40
	Total	104 (12.6%)	47 (11.3%)	145 (17.6%)	74 (17.8%)	**249 (30.2%)**	**121 (29.2%)**
SSG	Left	6	2	4	1	10	3
	Right	2	1	2	2	4	3
	Bilateral	0	0	0	0	0	0
	Total	8 (1,0%)	3 (0.7%)	6 (0.7%)	3 (0.7%)	**14 (1.7%)**	**6 (1.4%)**
CAC	Left	24	0	23	0	47	0
	Right	15	0	17	0	32	0
	Bilateral	6	0	8	1	14	1
	Total	45 (5.5%)	0 (0.0%)	48 (5.8%)	1 (0.2%)	**93 (11.3%)**	**1 (0.2%)**
CSL	Left	14	0	11	0	25	0
	Right	17	0	15	0	32	0
	Bilateral	6	0	9	0	15	0
	Total	37 (4.5%)	0 (0.0%)	35 (4.3%)	0 (0.0%)	**72 (8.8%)**	**0 (0.0%)**
IO	Left	25	24	36	33	61	57
	Right	31	26	28	29	59	55
	Bilateral	8	0	6	3	14	3
	Total	64 (7.8%)	50 (12.0%)	70 (8.5%)	65 (15.7%)	**134 (16.3%)**	**115 (27.7%)**

TL: tonsilloliths; SSG: sialoliths of the submandibular salivary gland; CAC: carotid artery calcifications, CSL: calcified submandibular lymph nodes; IO: idiopathic osteosclerosis; bold: summary.

volume images, and to verify that calcifications detected in the mandibular region on DPRs can be confirmed using 3D volume images.

2. Materials and methods

We retrospectively reviewed 822 DPRs with existing 3D volume images acquired for various reasons between 2013 and 2017 in the Danube Private University Department for Oral and Maxillofacial Surgery. Indications for the 3D volume images included implant planning, endodontic or orthodontic reasons, or evaluation of inflammation or anomalies.

Patients were eligible for inclusion in the study if they were 21–89 years old and had 3D images taken during their dental treatments. All radiographic images were acquired using the Orthophos SL 3D imaging unit (tube voltage: 60–90 kVp, tube current: 3–16 mA). A digital cadmium-telluride sensor with direct conversion sensor technology was used for the 2D images, and a digital flat-panel detector with an active sensor area of 160 × 160 mm was used for 3D imaging. In recent years, a ø5 × 5.5-cm FOV has been used in the clinic, with radiation doses of 3–20 μSv. All patients were positioned using a 3-point fixating system (Dentsply Sirona), whereby patients are required to bite on a specially designed device to ensure an ideal chin and forehead position. A light device determined the Frankfurt horizontal and mid-sagittal planes. The radiographs were viewed with Galileos Implants and Sidexis 4.0 software (Dentsply Sirona).

Two oral and maxillofacial surgeons and a dentist independently evaluated 822 DPRs for radiologic signs of calcification, particularly TL, IO, CAC, CSL, and SSG. The criterion for calcification was a localised radiopaque modular mass larger than 1 mm. A template created with publicly available digital image analysis software (GIMP 2.8.18, GNU Image Manipulation Program; http://gimp.org) was used. It included 10 fields representing the five predilection areas of calcification for each side [21]. Radiologic opacities representing CAC are located in the so-called "carotid artery territory," which is under the mandibular angle, next to the cervical vertebrae C3-C4. Suspicious calcifications were recorded as TL if they could be observed as single or multiple radiopacities over the oropharyngeal air space. CSL appear as single or multiple irregular opacities, usually in the submandibular region near the mandibular angle.

SSGs are frequently localized below the mandibular bone due to advanced mineralization and are often superimposed by the dental arch. IOs can be found between the roots or may be periapical (but separated from the teeth), with a high preference for the premolar/molar regions of the mandible. The DPRs were evaluated using a 15.6-inch B50-50 80S20006GE Notebook HD, Core i3-500 laptop (Lenovo, Morrisville, NC, USA) and an LG E2442 monitor with a resolution of 1920 × 1080 pixels (LG Electronics Austria GmbH, Vienna, Austria). The results were registered in Excel (Microsoft Corp., Redmond, WA, USA) and evaluated by two students. If an examiner detected one or more calcifications on a DPR, the 3D volume image was evaluated. Particular attention was paid to the mandible and the oral and vestibular spaces of the jaw to determine if calcifications detected on DPRs could be diagnosed on 3D volume images. Before the examination, the axial line of each 3D radiograph was adjusted to the mandibular comb, and the observation window was always set to the highest value of 50. This allowed the maximum range around the upper jaw to be inspected.

The results were graded according to the patients' sex and age, as well as where the calcification was diagnosed (left, right or bilateral). There were 10 fields in the Excel table (each calcification on both sides) with two categories: calcification detected or no calcification detected. In contrast to the DPRs, the 3D image data was organized based on the anatomical structures. The categories included no calcification diagnosed, calcification diagnosed, area could not be assessed, and range not assessed because the DPR showed no calcification (assigned to the patients for whom no 3D review took place).

Statistical analysis comparing the DPRs revealing one or more calcifications to the 3D images was performed using IBM SPSS Statistics software version 23.0 (IBM Corp., Armonk, NY, USA). The internal

Table 2
Evaluation of the distributions of calcifications on 3D images.

Parameter	TL	CAC	CSL	SSG	IO	Total
Area that could be evaluated on 3D images (%)	91.6	0.2	0.0	100	99.2	58.2
Compliance of diagnosed calcification between 3D images and DPR (%)	38.7	0.9	0.0	35.7	63.5	5.7
Areas with no correlation between DPR and 3D images (%)	48.1	0.1	0.0	64.3	34.5	5.6

3D: three-dimensional; TL: Tonsilloliths; CAC: carotid artery calcifications; CSL: calcified submandibular lymph nodes; SSG: sialoliths of the submandibular salivary gland; IO: idiopathic osteosclerosis; DPR: digital panoramic radiograph.

Fig. 1. This 3D image shows (A) panoramic, (B) axial, and (C) sagittal views of tonsilloliths.

reliability and age- and sex-dependence were evaluated using the chi-squared test and Fisher's exact test. P-values <0.05 were considered statistically significant.

The study protocol was approved by the lower Austria ethics review committee (approval number GS4-EK-4/379-2016).

3. Results

The 822 patients comprised 360 men (43.8%) and 462 women (56.2%), of whom 16.7% were 21–39 years old, 48.9% were 40–59, and 34.4% were 60–89. The images were divided into those for the right side and the left side. A minimum of one calcification was detected on the DPRs of 415 patients. The most common type of calcification detected was TL (n = 249, 30.2%), followed by IO (n = 134, 16.3%), CAC (n = 93, 11.3%), CSL (n = 72, 8.8%), and SSG (n = 14, 1.7%) (Table 1).

TL, CAC, and IO were more common in women, and SSG and CSL were more common in men. TL was the most common bilateral calcification; SSG and CAC were more likely to be on the left side, whereas CSL and IO were more likely to be on the right side. Distribution of the calcifications according to patients' age reveals that the group between 40–59 years was the most affected. Only 287 calcifications on the 415 DPRs were validated on 3D volume images (Table 2).

Fig. 2. This 3D image shows (A) panoramic, (B) axial, and (C) sagittal views of a sialolith of the submandibular gland.

Fig. 3. This 3D image shows (A) panoramic, (B) axial, and (C) sagittal views of a calcified atherosclerotic plaque.

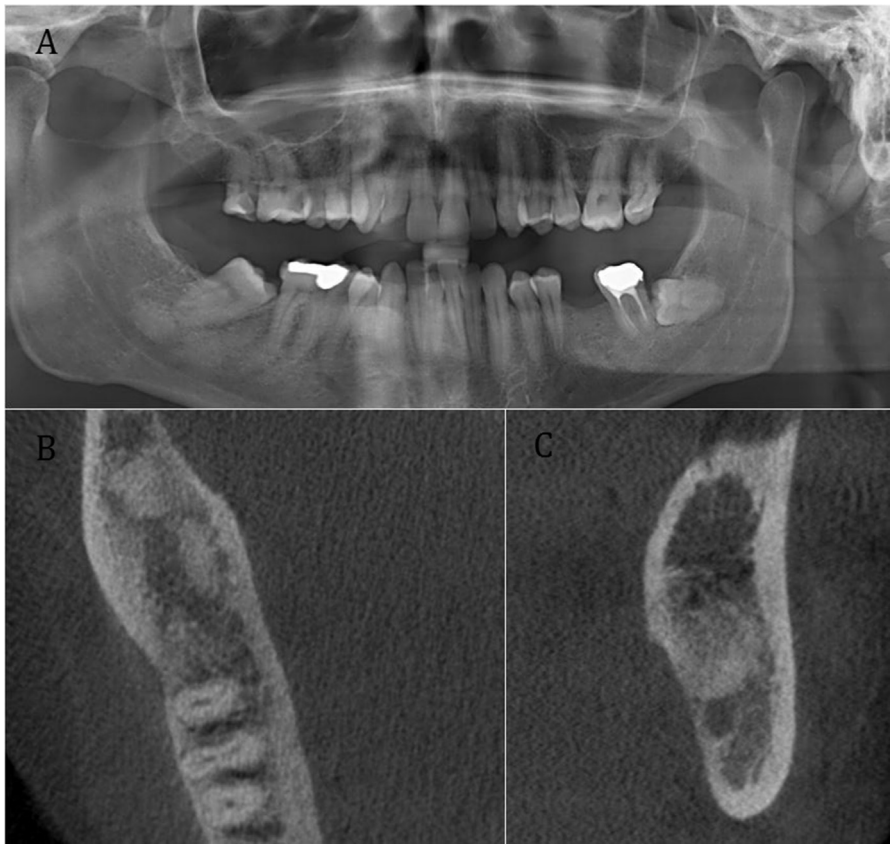

Fig. 4. This 3D image shows (A) panoramic, (B) axial, and (C) sagittal views of idiopathic osteosclerosis.

The calcifications most commonly confirmed were TL (n = 121, 29.2%), followed by IO (n = 115, 27.7%), SSG (n = 6, 1.4%), and CAC (n = 1, 0.2%). No CSLs were confirmed. TL, CAC, and IO were confirmed on 3D volume images more often in women, although there was no sex differences for SSG or CSL. TL was more likely to be confirmed on the right side, and IO and CAC were more likely to be confirmed on the left side. SSG and CSL occurred with equal frequency on both sides. There was wide variation in the degree of agreement between the types of calcification detected on DPR and confirmed on 3D volume images (Table 2).

There was an accordance of 38.7% between TL diagnosed on the 3D volume images and those diagnosed on the DPRs. Of the TL diagnosed on

the 3D volume images, 87.0% were previously detected on the DPRs. Because this was a retrospective study and the focus field of the 3D volume images varied, 8.4% of the areas were not observable on the 3D images. There was an accordance of 35.7% between SSG diagnosed on the 3D volume images and those diagnosed on the DPRs. Of the SSG diagnosed on the 3D volume images, 83.3% were previously detected on the DPRs.

In the majority of cases, there was confusion between SSG and IO on the DPRs. In terms of calcified atherosclerotic plaque, there was an accordance of 0.9 % between diagnosed CAC on the 3D images and previously diagnosed CAC on the DPR. Of CAC diagnosed on the 3D images, 50.0% could previously be detected on the DPR. There was no accordance in regard to CSL, because none could be detected in the 3D volume images. There was an accordance of 63.5 % between diagnosed IO on the 3D volume images and previously diagnosed IO on the DPR. Of the IO diagnosed on the 3D images, 79.7% could previously be detected on the DPR.

4. Discussion

Numerous researchers have attempted to improve the ratio of the maximal 3D range to the lowest possible radiation emission in CBCT and to validate their results using CT [16]. However, in this study, we used the Orthophos SL 3D device to evaluate the potential of 3D radiography as a reliable imaging technique for the detection of calcifications in the head and neck region. The technique can be used to obtain images of the jaw and a limited area of the surrounding bone. Whereas previous research has focused on incidental CBCT findings [4], we focused on the diagnostic process, which begins with a DPR and proceeds to 3D imaging in some cases. The DPR is still the diagnostic method of choice [6], although the type of 3D imaging that should be used in the next step remains unclear. Our diagnostic range was less than that reported by Togan et al. [4], who examined 999 CBCT images using the 3D eXam CBCT scanner (KaVo Dental GmbH, Biberach, Germany) at 90–120 kVp and 3–8 mA. Chambers et al. [11] evaluated the dose required for CBCT using the Galileos system. They found that a reduced dose led to a decreased FOV, and changes in the tube current and beam collimation had a significant impact on the required dose. If the setting is changed for 3D imaging in the future, the results may deviate considerably from those reported so far. Early diagnosis of soft tissue calcification is not important in many cases, but in others, it may be life-saving. Patients with CAC have an increased risk of stroke and should be referred to a specialist. In contrast, IO would not require further treatment. However, first we need to distinguish between the different types of calcifications. There is no disadvantage to early diagnosis.

TLs (Fig. 1) are small dystrophic structures predominantly located in the tonsillar crypts. They may cause dysphagia, chronic inflammation in the throat, earache, and halitosis. Whether this type of calcification becomes symptomatic depends on its size and location. In our study, the prevalence of TL on DPRs was 30.2%, whereas another study that examined the prevalence of TL on 2000 DPRs reported a prevalence of 5.05% [9]. Further, we found a prevalence of 29.2% of TL on 3D volume images, which is similar to the prevalence of 24.6% found in another study that examined 150 CT images [22]. The concordance of TL diagnosed on DPR and 3D volume images was only 38.7%, possibly because 13.7% of cases could not be evaluated, and 48.1% of cases were falsely diagnosed on DPRs or confused with IO. Oda [23] compared the TL detection rates between DPRs and CT scans, and found a rate of only 7.3% on DPRs. The reason for this low detection rate was the size of the TL; the smaller the TL, the lower the detection rate on DPR.

Sialolithiasis refers to the accumulation of inorganic deposits, predominantly calcium phosphate, in the salivary glands (Fig. 2) or salivary processes [1, 3]. Of the 14 SSGs diagnosed on DPR, 35.7% were confirmed on 3D volume images. The fact that this area could always be evaluated suggests that 3D volume radiography is an appropriate method of confirmation for this type of calcification.

The internal carotid artery is the most common site of atherosclerotic plaque (Fig. 3). CAC increases the risk of vasoconstriction, which can progress to occlusion. Patients with CAC are at an increased risk for cerebral infarction, so early diagnosis is essential. In our study, only one case of CAC was detected with 3D imaging; hence, the prevalence of CAC was 0.9%. This is much lower than in another study that evaluated incidental CBCT findings, which reported a prevalence of 5.3% [4]. However, in our study, 99.1% of the 3D volume images could not evaluate the area containing the internal carotid artery. Changing the FOV of 3D X-ray taken in the future may be beneficial.

This is also true in regard to the diagnosis of CSL. We found that the prevalence of these calcifications was 8.8% on DPRs, but none of these areas could be assessed with 3D volume images.

IO is not a calcification of soft tissue (Fig. 4), but it is the main differential diagnosis of soft tissue calcification in the mandibular region on DPR [24]. IO is an unusual area of increased bone density and does not require immediate treatment. However, these lesions tend to occur in more than one region of the body. The concordance rate between the DPRs and 3D volume images was 63.5%, the highest for this type of calcification.

The prevalence of calcifications increases with age. Over 80% of the calcifications were found in patients older than 40. No significant difference was found in relation to patient sex or whether the calcification was on the left or right side.

5. Conclusion

The DPR may be used for the early diagnosis of IO, but in order to clarify the findings, more detailed imaging is necessary. 3D volume images may be a good choice to diagnose TL, SSG, and IO, as they can more accurately determine the location than DPRs. Calcifications in the mandibular region such as TL, SSG, and IO can be evaluated on 3D volume images with a low FOV and a radiation dose of 3–16 mA, whereas CAC and CSL require a greater FOV and probably a higher radiation dose.

Declarations

Author contribution statement

Barbara Schreiner-Tiefenbacher: Conceived and designed the experiments; Performed the experiments; Wrote the paper.

Walter Sutter, Marius Meier: Performed the experiments; Analyzed and interpreted the data.

Vivian Forster: Conceived and designed the experiments; Performed the experiments.

Klaudio Pauli: Conceived and designed the experiments.

Dritan Turhani: Performed the experiments; Analyzed and interpreted the data; Contributed reagents, materials, analysis tools or data.

Funding statement

This research did not receive any specific grant from funding agencies in the public, commercial, or not-for-profit sectors.

Competing interest statement

The authors declare no conflict of interest.

Additional information

No additional information is available for this paper.

Acknowledgements

The authors would like to thank Univ. Prof. Mag. Dr. PhDr. Wilhelm Frank MLS for the statistical analyses.

References

[1] F. Caglayan, M. Akif Sümbüllü, O. Miloglu, H.M. Akgül, Are all soft tissue calcifications detected by Cone-beam computed tomography in the submandibular region sialoliths? J. Oral Maxillofac. Surg. 72 (2014) 1531.

[2] A.D. Soares, A.M. Wanzeler, M.D. Oliveria Renda, C.G. Marinho, F.M. Tuji, Cone-Beam computed tomography findings in the early diagnosis of calcified atheromas, J. Oral Maxillofac. Surg. 75 (2017) 143–148.

[3] E.H. Van der Meij, K.H. Karagozoglu, J.G.A.M. De Visscher, The value of cone-beam computed tomography in the detection of salivary stones prior to sialendoscopy, J. Oral Maxillofac. Surg. 47 (2017) 223–227.

[4] B. Togan, T. Gander, M. Lanzer, R. Martin, H.T. Lübbers, Incidence and frequency of nondental incidental findings on cone-beam computed tomography, J. Cranio-Maxillo-Fac. Surg. 44 (2016) 1373–1380.

[5] L. Khojastepour, A. Haghnegahdar, H. Sayar, Prevalence of soft tissue calcifications in CBCT images of mandibular region, J. Dent. 2 (2017) 88–94.

[6] J. Vengalath, J.H. Puttabuddi, B. Rajkumar, G.C. Shivakumar, Prevalence of soft tissue calcifications on digital panoramic radiographs: a retrospective study, J. Indian Acad. Oral Med. Radiol. 26 (2014) 385–389.

[7] N. Khambete, R. Kumar, M. Risbud, A. Joshi, Reliability of digital panoramic radiographs in detecting calcified carotid artery atheromatous plaques: a clinical study, Indian J. Dent. Res. 25 (2014) 36–40.

[8] I. Garay, H.D. Netto, S. Olate, Soft tissue calcified in mandibular angle area observed by means of panoramic radiography, Int. J. Clin. Exp. Med. 7 (2014) 51–56.

[9] J. Ghabanchi, A. Haghnegahdar, L. Khojastehpour, A. Ebrahimi, Frequency of tonsilloliths in panoramic views of a selected population in southern Iran, J. Dent. 16 (2015) 75–80.

[10] G. Deeb, L. Antonos, S. Tack, C. Carrico, D. Laskin, J.G. Deeb, Is Cone-beam computed tomography always necessary for dental implant placement? J. Oral Maxillofac. Surg. 72 (2016) 285–289.

[11] D. Chambers, R. Bohay, L. Kaci, R. Barnett, J. Battista, The effective dose of different scanning protocols using the Sirona Galileos comfort CBCT scanner, Dentomaxillofacial Radiol. 44 (2015) 2.

[12] R. Boeddinghaus, A. Whyte, Trends in maxillofacial imaging, Clin. Radiol. 73 (2018) 4–18.

[13] S. Saati, F. Kaveh, S. Yarmohommadi, Comparison of cone beam computed tomography and multi slice computed tomography image quality of human dried mandible using 10 landmarks, J. Clin. Diagn. Res. 11 (2017) ZC13–ZC16.

[14] A. Gracco, A. De Stefani, G. Bruno, P. Balasso, G. Alessandri-Bonetti, E. Stellini, Elongated styloid process evaluation on digital panoramic radiograph in a North Italian population, J Clin Exp Dent 9 (2017) 400–404.

[15] B. Feragalli, O. Rampado, C. Abate, M. Macrì, F. Festa, F. Stromei, et al., Cone beam computed tomography for dental and maxillofacial imaging: technique improvement and low-dose protocols, Radiol. Med. 122 (2017) 581–588.

[16] R.A. Katkar, C. Kummmet, D. Dawson, L. Moreno Uribe, V. Allareddy, M. Finkelstein, et al., Comparison of observer reliability of three-dimensional celometric landmark identification on subject images from Galileos and i-cat cone beam CT, Dentomaxillofacial Radiol. 42 (2013) 20130059.

[17] S.D. Reiz, J. Neugebauer, V.E. Karapetian, L. Ritter, Cerec meets Galileos–integrated implantology for completely virtual implant planning, Int. J. Comput. Dent. 17 (2014) 145–157.

[18] Y. Daniz, G. Geduk, A.Z. Zengin, Examination of foramen tympanicum: an anatomical study using cone-beam computed tomography, Folia Morphol. 77 (2018) 335–339.

[19] S.L. Kabak, N.V. Zhuravleva, Y.M. Melnichenko, N.A. Savrasova, Study of the mandibular incisive canal anatomy using cone beam computed tomography, Surg. Radiol. Anat. 39 (2017) 647–655.

[20] M. Stimmelmayr, K. Denk, K. Erdelt, G. Krennmair, S. Mansour, F. Beuer, et al., Accuracy and reproducibility of four cone beam computed tomography devices using 3D implant-planning software, Int. J. Comput. Dent. 6 (2017) 21–34.

[21] W. Sutter, S. Berger, M. Meier, A. Kropp, A.M. Kielbassa, D. Turhani, Cross-sectional study on the prevalence of carotid artery calcifications, tonsilloliths, calcified submandibular lymph nodes, sialoliths of the submandibular gland, and idiopathic osteosclerosis using digital panoramic radiography in a Lower Austrian subpopulation, Quintessence Int. 22 (2018), 231-24.

[22] M.A. Fauroux, C. Mas, P. Tramini, J.H. Torres, Prevalence of palatine tonsilloliths: a retrospective study on 150 consecutive CT examinations, Dentomaxillofacial Radiol. 42 (2013) 20120429.

[23] M. Oda, S. Kito, T. Tanaka, I. Nishida, S. Awano, Y. Fujita, et al., Prevalence and imaging characteristics of detectable tonsilloliths on 482 of consecutive CT and panoramic radiographs, BMC Oral Health 13 (2013) 54.

[24] U. Gianelli, S. Fiori, D. Cattaneo, A. Bossi, I. Cortinovis, A. Bonometti, et al., Prognostic significance of a comprehensive histological evaluation of reticulin fibrosis, collagen deposition and osteosclerosis in primary myelofibrosis patients, Histopathology 71 (2017) 897–908.